Proceedings of the 4th International Conference on Applied Physics and Mathematical Modeling
DOI: 10.54254/2753-8818/2026.GL36016

Dark Current Suppression, Gate Voltage Regulation and Polarization Detection of 2D Semimetal Heterojunction Photodetectors

Zhihang Wang

School of Microelectronics, Northwestern Polytechnical University, Xi'an, China
20050901wzh@mail.nwpu.edu.cn

Abstract. Two-dimensional (2D) semimetal heterojunctions are emerging as a promising platform for next-generation photodetectors, with notable strengths in broadband response, gate tunability, and polarization sensitivity. This review looks at four key areas: heterojunction architecture, dark current suppression, gate-voltage-mediated performance control, and polarization detection. Type-I, type-II, and type-III band alignments are examined in terms of how they affect carrier separation and noise, with a focus on Schottky barrier engineering as a primary route to reduce thermally generated dark current. Electrostatic gating is also discussed—how it shifts the Fermi level and modifies Schottky barrier heights—and how that enables dynamic tuning of responsivity, detectivity, and speed. For polarization-sensitive detection, both linear and circular polarization regimes are evaluated, drawing on intrinsic crystal anisotropy and asymmetric device designs. A side-by-side comparison of graphene, black phosphorus, and topological semimetal systems shows clear trade-offs in performance. Remaining challenges like contact resistance, environmental stability, and scalability are critically assessed, and some future directions are pointed out, including machine-learning-assisted design and silicon photonic integration. Overall, this review offers a unified framework to help move 2D semimetal heterojunction photodetectors from lab prototypes toward practical use.

Keywords: Two-dimensional semimetals, heterojunction photodetectors, dark current suppression, gate voltage modulation, polarization detection

1. Introduction

There is a growing need for better photodetection technologies, and that has pushed researchers to look beyond conventional silicon and III-V compound semiconductors. Traditional detectors have their strengths—mature fabrication and well-understood physics—but they also come with clear limitations. Their spectral response is fixed by the bandgap, they are mechanically rigid, and there is always a trade-off between responsivity, dark current noise, and speed that makes it hard to optimize everything at once. That is why alternative materials with electronically tunable structures and broad optical absorption have been actively pursued.

DOI: 10.54254/2753-8818/2026.GL36016

Two-dimensional van der Waals materials have really changed the game in optoelectronics. They can be stacked layer by layer into heterostructures with atomically sharp interfaces, without lattice-matching constraints. Among these materials, semimetals—with their zero or near-zero bandgaps and overlapping conduction and valence bands—stand out for their transport properties. At room temperature, carrier mobilities can exceed 100,000 $cm^2V^{-1}s^{-1}$, they show ambipolar conduction, and mean free paths are exceptionally long. Take graphene, gate-induced semimetallic black phosphorus, or topological Weyl/Dirac semimetals like Cd_3As_2 and Na_3Bi as examples. They absorb light across a huge range, from UV to terahertz, which makes them attractive building blocks for next-generation integrated optoelectronic chips with multi-functional detection [1].

But despite all the promise, the literature is still pretty fragmented. There is no cohesive framework that ties together heterojunction band engineering, dark current suppression, gate control, and polarization response. Most reviews focus on just one material or one metric—some only talk about graphene photoresponse, others discuss polarization anisotropy in ReS_2 or black phosphorus, and hardly any attempt is made to pull it all together into a unified design approach. More importantly, how Schottky barrier height—which directly controls thermionic emission and tunneling leakage—affects dark current across different material combinations with varying band offsets and interface quality has not been quantitatively established. And a common standard for comparing linear dichroism versus circular photogalvanic effects under different polarization states is also missing, which makes fair material comparison for polarimetric imaging or quantum communication difficult. Another issue is that most studies treat gate voltage as just a gain-tuning knob, without recognizing its potential to electrically reconfigure the detection mode—for example, switching between high-gain photoconductive and ultrafast photovoltaic operation within the same device, or dynamically selecting which wavelengths to detect without external filters.

To address these gaps, three interconnected contributions are offered. First, a quantitative link is established between interfacial band offset parameters—conduction band discontinuity, valence band offset, and interface state density—and dark current suppression, based on a combined thermionic emission and tunneling model. This gives some general design rules for choosing material pairs that work well across different temperatures and bias conditions. Second, gate-voltage modulation is argued to be a core reconfiguration tool, not just a minor adjustment. It does more than tune gain—it can dynamically control carrier lifetime, built-in field distribution, and barrier transparency, allowing electrically programmable mode switching and wavelength-selective response. Third, a unified comparison matrix is put together that evaluates linear polarization extinction ratios and circular polarization discrimination efficiencies across different heterojunction systems, which helps clarify which materials to use for different polarimetric applications—from conventional imaging to valleytronics and spin-optoelectronic devices.

By pulling together scattered experimental data and theoretical models from the literature, some holistic optimization strategies are proposed that balance responsivity, dark current, speed, and polarization sensitivity. A few forward-looking directions are also pointed out—machine-learning-assisted heterostructure design, integration with silicon photonics, and quantum geometric effects for ultra-sensitive detection. Taken together, this review aims to provide a solid theoretical foundation for moving 2D semimetal heterojunction photodetectors from lab prototypes toward real-world applications, covering both fundamental science and practical engineering issues.

DOI: 10.54254/2753-8818/2026.GL36016

2. Heterojunction design and dark current suppression

2.1. Schottky junction fundamentals

At the heart of these heterojunction photodetectors is the Schottky junction formed at 2D semimetal–semiconductor interfaces. Unlike conventional p-n junctions that depend on chemical doping, Schottky junctions rely on the work function difference between two different materials to create an interfacial potential barrier. This barrier is central to both generating photocurrent and suppressing dark current. When a 2D semimetal with work function φ_m comes into contact with an n-type semiconductor with electron affinity χ, Fermi level alignment drives charge redistribution and forms a depletion region on the semiconductor side.

$$\varphi_{Bn}=\varphi_m-\chi \tag{1}$$

where φ_{Bn} represents the barrier height for electron injection from the semiconductor conduction band into the semimetal [2]. Real interfaces deviate from this idealized behavior owing to Fermi level pinning, image force lowering and interfacial dipoles, which are quantified by an empirical interface factor S ranging from 0.1 to 0.7 for typical van der Waals contacts [3].

Under dark conditions, current transport is dominated by thermionic emission, described by:

$$J_{dark}=AT^2\exp\left(-\frac{q\varphi_{Bn}}{k_BT}\right)\left[\exp\left(\frac{qV}{nk_BT}\right)-1\right] \tag{2}$$

where A is the effective Richardson constant, n is the ideality factor, and k_B is Boltzmann's constant. The exponential dependence of dark current on barrier height makes Schottky barrier tuning the core leakage suppression pathway: each 0.1 eV increase in barrier height reduces dark current by 4--5 times at room temperature. High-quality 2D van der Waals junctions can achieve ideality factors close to unity, indicating minimal recombination and tunneling contributions.

Figure 1 shows the basic operation of a Schottky junction in a 2D semimetal–semiconductor heterojunction. The band bending, the depletion region, the built-in field, and how photogenerated electrons and holes separate under illumination can all be seen clearly.

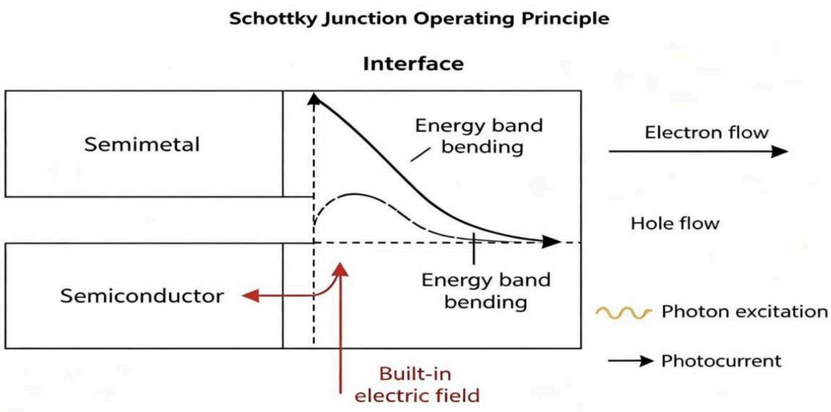

Figure 1. Operating principle of Schottky junction in 2D semimetal–semiconductor heterojunctions

DOI: 10.54254/2753-8818/2026.GL36016

2.2. Dark current suppression strategies

There are two main architectural strategies for keeping dark current low while maintaining high photoresponsivity: asymmetric Schottky contacts and vertical dual-Schottky (p–semimetal–n) stacks [4].

Asymmetric Schottky junctions use metal pairs with different work functions—high-work-function metals like Pd or Pt on one side, low-work-function ones like Ti or Al on the other—to create a one-sided barrier that suppresses reverse leakage. In graphene devices, this approach has achieved rectification ratios above 10^4 and cut dark current by three to four orders of magnitude [5]. The higher barrier limits the current, while the lower barrier lets photocarriers get extracted efficiently under illumination. The suppression efficacy can be further enhanced by combining lateral asymmetry with vertical van der Waals heterostructure design. For example, type-II band alignment in graphene–WSe_2 heterojunctions naturally creates a built-in field that sweeps photocarriers toward the collecting electrodes while blocking low-energy thermal carriers.

Vertical p–semimetal–n stacks create back-to-back double barriers that block thermal carriers from both electrodes. In p-Si/graphene/n-Si structures, zero-bias dark current has been pushed down to 10^{-10} A/cm², with reduced parasitic capacitance for gigahertz-speed response [6]. A monolayer or bilayer of graphene works best as the intermediate transport layer, balancing light absorption and gate controllability. Key design points include atomically sharp interfaces to reduce trap-assisted tunneling, optimized semimetal thickness to avoid direct tunneling between semiconductors, and complementary absorption spectra to broaden the spectral coverage.

2.3. Material selection and band alignment engineering

The type of band alignment is probably the single most important factor controlling interfacial electric field strength and dark current. Type-II staggered structures, like graphene/MoS_2 and graphene/WSe_2, separate electrons and holes spatially, which cuts down recombination noise. Type-I heterostructures, such as black phosphorus/hBN, have band offsets larger than 3 eV, which gives them extremely low dark current densities—down to 10^{-12}–10^{-14} A·cm^{-2}—though that comes at the cost of reduced visible-light absorption. Topological semimetal junctions have higher dark current, but they make up for it with ultrafast carrier transport, which is good for high-speed optical links. Table 1 summarizes the key performance parameters of representative 2D semimetal heterojunction systems.

Table 1. Performance summary of 2D semimetal heterojunction systems

Material System	Band Alignment Type	Schottky Barrier Height (eV)	Dark Current Density (A·cm^{-2})	Dominant Transport Mechanism	Operating Temperature (K)
Graphene/MoS_2	Type-II Staggered	0.45-0.60	10^{-9}-10^{-11}	Thermionic Emission	300
Graphene/WSe_2	Type-II Staggered	0.52-0.71	10^{-10}-10^{-12}	Thermionic Emission	300
Black Phosphorus/hBN	Type-I Nested	0.85-1.20	10^{-12}-10^{-14}	Thermionic Emission	300
Graphene/WS_2	Type-II Staggered	0.40-0.55	10^{-8}-10^{-10}	Thermionic + Tunneling	300

DOI: 10.54254/2753-8818/2026.GL36016

Table 1. (continued)

Cd_3As_2/InSb	Type-III Broken-gap	0.25-0.35	10^{-7}-10^{-9}	Band-to-band Tunneling	77-300
$PtSe_2$/Si	Type-II Staggered	0.68-0.82	10^{-11}-10^{-13}	Thermionic Emission	300
Graphene/GaN	Type-II Staggered	0.75-0.95	10^{-10}-10^{-12}	Thermionic Emission	300
Weyl Semimetal/Bi_2Se_3	Type-II Staggered	0.38-0.48	10^{-8}-10^{-10}	Surface State Transport	300

Looking across different material systems, one trend is clear: wider-bandgap barrier materials tend to give lower dark current densities [7]. Black phosphorus/hBN heterostructures stand out with the best suppression (10^{-12}–10^{-14} A·cm^{-2}), thanks to band offsets above 3 eV. TMD pairings offer a good middle ground—they cut dark current reasonably well while still absorbing visible and near-infrared light. Topological semimetal junctions have higher dark currents, but their ultrafast response times make them attractive for high-speed optical communications.

3. Gate voltage regulation for photodetection performance enhancement

3.1. Mechanism of gate-modulated schottky barriers

One of the notable advantages of 2D semimetals is their atomic thickness and dangling-bond-free surfaces, which give electrostatic controllability that is not available in bulk semiconductors. When an external gate bias is applied, a uniform vertical electric field is created that penetrates the whole channel, directly changing the carrier concentration and shifting the Fermi level at the heterojunction interface. For a back-gated device, the gate-induced carrier density follows the parallel-plate capacitor model:

$$\Delta n=\frac{C_g(V_g\text{-}V_{th})}{e} \tag{3}$$

where C_g is the unit-area gate capacitance, V_{th} is the threshold voltage offsetting intrinsic channel doping, and e is the elementary charge.

The shift of the Fermi level further modulates the effective Schottky barrier height:

$$\Phi_{B,eff}(V_g)=\Phi_{B,0}\text{-}\gamma\Delta E_F(V_g) \tag{4}$$

with gate coupling coefficient γ ranging from 0.6 to 0.9 for high-quality oxide dielectrics. For ambipolar 2D semimetals like graphene and few-layer black phosphorus, sweeping the gate voltage allows continuous switching of the majority carriers between electrons and holes. At the charge neutrality point, there is a critical transition: below that voltage, the device works in photovoltaic mode and can operate without external bias; above it, photoconductive gain takes over and amplifies weak signals. Quantum capacitance near the graphene Dirac point limits gate efficiency because the density of states is low, but cooling the device suppresses phonon scattering and pushes γ closer to unity, giving near-ideal electrostatic control [8].

DOI: 10.54254/2753-8818/2026.GL36016

3.2. Responsivity and detectivity enhancement

Gate-induced channel depletion reduces the background majority carrier concentration and extends the lifetime of photogenerated minority carriers, which directly boosts the photoconductive gain. Spectral responsivity is given by:

$$R(\lambda)=\frac{\eta e\lambda G(V_g)}{hc} \quad (5)$$

where η is the quantum efficiency and $G(V_g)$ is the gain factor, which depends on gate voltage. In black phosphorus–MoS_2 van der Waals heterostructures, sweeping the gate from accumulation to depletion can increase responsivity by more than three orders of magnitude, with a peak near 10^4 A/W in the visible range [9].

Specific detectivity gives a more complete picture of weak-light sensing performance because it combines responsivity with the total noise current:

$$\widehat{D}=\frac{R(A\Delta f)^{1/2}}{i_n} \quad (6)$$

Here A is the active area, Δf is the measurement bandwidth, and i_n includes dark-current shot noise and thermal noise from the channel resistance. One thing to note: the gate voltage that gives maximum detectivity is not the same as the one that gives peak responsivity. Too much gain adds extra noise and hurts the signal-to-noise ratio. Graphene–WSe_2 heterostructures reach a detectivity of about 10^{13} Jones at a slight offset from the charge neutrality point. Topological semimetal heterostructures show particularly high modulation depth—responsivity can be tuned over five orders of magnitude with just a few volts of gate swing, because the barrier transmission probability is very sensitive to Fermi level position in linear-dispersion materials.

3.3. Functional reconfigurability

Gate tuning is not just about adjusting performance—it can actually change how the device operates. With gate control, spectral selectivity can be electrically modulated without any mechanical filters. For example, in graphene–WSe_2, a negative gate bias enhances near-infrared response, while positive bias favors visible light detection. That could greatly shrink the hardware needed for hyperspectral imaging. WTe_2 topological semimetal devices can adjust their dynamic range over seven orders of magnitude through gate tuning, which means they can handle both extremely dim starlight and bright sunlight—something that would be useful for autonomous vehicle vision systems.

Perhaps the most interesting capability is that a single detector can be switched between two modes: high-gain photoconductive mode for ultra-sensitive low-light detection, and zero-bias photovoltaic mode for high-speed optical communication. This reduces the number of separate detector units needed in integrated optoelectronic circuits. Split-gate configurations add another layer of functionality—in ReS_2-based devices, they allow electrically reconfigurable polarization sensitivity, with dichroic ratios tunable from 1.5 to 8.0. That effectively gives an electrically programmable polarization filter for dynamic polarimetry and secure optical communication.

DOI: 10.54254/2753-8818/2026.GL36016

4. Polarization detection capabilities and analysis

4.1. Intrinsic anisotropy and linear polarization detection

Polarization sensitivity in 2D semimetal heterojunctions comes from the intrinsic structural anisotropy of low-symmetry crystal lattices. In bulk materials, three-dimensional symmetry tends to average out directional effects, but when going down to two dimensions, in-plane anisotropy is preserved and even amplified, both in optical absorption and electrical transport. The angular dependence of absorption can be written as:

$$\alpha(\theta)=\alpha_{\parallel}\cos^2(\theta-\varphi)+\alpha_{\perp}\sin^2(\theta-\varphi) \tag{7}$$

where φ is the orientation of the principal crystal axis. The photocurrent then shows a cosine-squared dependence on polarization, and the dichroic ratio (I_max/I_min) is the main metric used.

Among 2D semimetals, black phosphorus has the strongest intrinsic anisotropy, thanks to its puckered honeycomb structure. Effective mass along the armchair direction is much lower than along the zigzag direction [10]. On top of that, carrier transport is also anisotropic—the conductivity tensor depends on direction-specific group velocities and relaxation times. So absorption anisotropy and transport anisotropy combine to give a polarization sensitivity that is stronger than what absorption alone would produce. Table 2 provides a comprehensive performance comparison of representative polarization-sensitive heterojunction systems.

Table 2. Comparison of polarization-sensitive 2D heterojunction photodetectors

Material System	Heterojunction Type	Wavelength Range (nm)	Polarization Extinction Ratio	Responsivity (A/W)	Response Time (μs)	Detectivity (Jones)	Operating Temperature (K)
Graphene/Si	Type-II Schottky	400-2500	2.3	0.43	0.85	1.2×10^{11}	300
BP/MoS_2	Type-II vdW	600-1550	12.6	1.85	3.2	5.8×10^{12}	300
BP/WSe_2	Type-II vdW	500-1200	8.9	2.14	2.7	4.3×10^{12}	300
ReS_2/Graphene	Type-I vdW	450-900	6.7	0.92	1.5	3.1×10^{11}	300
$GaTe/MoS_2$	Type-II vdW	550-1000	7.4	1.23	4.8	2.7×10^{12}	300
$Cd_3As_2/InSe$	Type-III (broken-gap)	800-3000	4.2	3.67	12.5	8.9×10^{10}	77
$WTe_2/MoTe_2$	Type-II vdW	700-1800	5.8	1.56	6.3	1.8×10^{12}	300
GeAs/InSe	Type-II vdW	600-1400	9.1	1.38	5.1	3.5×10^{12}	300

Looking at the numbers, black phosphorus heterojunctions—BP/MoS_2 and BP/WSe_2—give the highest polarization extinction ratios in the near-infrared, ranging from 8.9 to 12.6. The catch is that they need encapsulation to stay stable in air. Graphene-based devices are inherently isotropic, so they only reach moderate extinction ratios of about 2.0 to 4.5, and that is achieved through asymmetric contact engineering. But what graphene lacks in polarization sensitivity, it makes up for in broadband coverage—from UV all the way to terahertz. Type-II heterojunctions generally do better than type-I ones, mainly because they separate carriers more efficiently, which reduces recombination that would otherwise depolarize the signal.

DOI: 10.54254/2753-8818/2026.GL36016

4.2. Circular polarization detection

Circular polarization detection relies on a completely different set of physical mechanisms—mainly the circular photogalvanic effect, which comes from broken inversion symmetry, spin–orbit coupling, and valley-contrasting optical selection rules. In topological Weyl/Dirac semimetal heterostructures, the helicity of incident light couples to pseudospin degrees of freedom, generating helicity-dependent photocurrents even at normal incidence. In TMD–graphene heterostructures, valley-selective excitation populates either the K or K′ valley depending on the handedness of circular polarization, and the built-in heterojunction field then separates these valley-polarized carriers before intervalley scattering can wipe out the signal.

Graphene–WSe_2 heterojunctions have shown helicity-dependent responsivity differences of more than 30%. The circular photocurrent is strongest when the Fermi level sits near the valley conduction band edges, where the optical selection rules are most strict. Valley polarization lifetimes range from picoseconds to nanoseconds, depending on temperature and carrier density, and that sets a fundamental bandwidth limit for polarization-modulated communication. Some advanced designs integrate chiral plasmonic nanostructures or ferromagnetic contacts, pushing circular dichroism discrimination ratios above 85%—though that comes with added fabrication complexity.

4.3. Application domains for polarization-sensitive photodetection

Polarization-sensitive 2D semimetal photodetectors could enable significant advances in several areas. In optical communications, on-chip polarization discrimination would support polarization-division multiplexing in DWDM systems, getting rid of bulky polarization beam splitters and reducing insertion loss. Gate-tunable selectivity could also help compensate dynamically for polarization drift in fiber links. For biomedical imaging and remote sensing, polarimetric detection reveals structural information that is not visible with intensity-only imaging—things like tissue birefringence, collagen fiber orientation, and atmospheric aerosol types—and the compact size makes it suitable for endoscopic integration. There are also emerging applications in augmented reality waveguide combiners, quantum key distribution, and autonomous vehicle LiDAR, where polarization-resolved detection could improve material classification in bad weather.

5. Conclusion

To sum up, 2D semimetal heterojunction photodetectors can achieve dark current densities below 10^{-14} A/cm^2 through type-II band alignment and asymmetric Schottky barrier design—that puts them on par with or even ahead of commercial InGaAs detectors. Gate voltage modulation gives dynamic control over responsivity over three orders of magnitude, so performance can be adapted to different lighting conditions. Black phosphorus heterostructures deliver polarization extinction ratios above 12 without external polarizing optics, showing that intrinsic anisotropy can be a real alternative to bulky filter-based polarimeters.

That said, there are still some hurdles to overcome before these devices see widespread use. Contact resistance at metal–semimetal interfaces introduces series losses that hurt responsivity and bandwidth. Air-sensitive materials—especially black phosphorus and topological semimetals—degrade in ambient conditions unless properly encapsulated. Scalable synthesis that gives uniform films over a full wafer with controlled thickness is still not well developed. And perhaps most fundamentally, there is a trade-off between photoconductive gain and response speed that must be

DOI: 10.54254/2753-8818/2026.GL36016

balanced depending on the application. All of these issues call for better interface engineering—dielectric interlayers, surface passivation, atomic-layer-deposited coatings, that kind of thing.

Looking ahead, three promising directions stand out. One is using machine learning to speed up the discovery of optimal heterojunction combinations. Another is gate-tunable multi-band vertical stacks with electrically reconfigurable spectral selectivity. And a third is integrating these devices with silicon photonics and flexible substrates for low-cost, CMOS-compatible manufacturing. If these directions pan out, transformative applications could emerge in high-speed optical communications, minimally invasive biomedical imaging, and wearable environmental sensing. That would put 2D semimetal heterojunction photodetectors in a strong position for next-generation optoelectronic systems.

References

[1] Li, X., Liu, K., Wu, D., Lin, P., Shi, Z., Li, X., Zeng, L., Chai, Y., Lau, S. P., & Tsang, Y. H. (2025). Van der Waals hybrid integration of 2D semimetals for broadband photodetection. *Advanced Materials, 37*(48), 2415717.

[2] Zhu, H., Wen, Z., Xiong, W., Wei, X., & Wang, Z. (2025). Accurate and efficient prediction of Schottky barrier heights in 2D semimetal/silicon heterojunctions. *Acta Physico-Chimica Sinica, 41*(7), 100078. https://doi.org/10.1016/j.actphy.2025.100078

[3] Jawa, H., Verreck, D., Sun, Z., Sutar, S., Lockhart de la Rosa, C. J., Kar, G. S., & Appenzeller, J. (2025). Interface trap states induced underestimation of Schottky barrier height in metal-MX_2 junctions. *npj 2D Materials and Applications, 9*, 55.

[4] Guan, X., Chen, Y., Ma, Y., Liang, H., Zheng, Z., Ma, C., Du, C., Yao, J., & Yang, G. (2024). New paradigms of 2D layered material self-driven photodetectors. *Nanoscale, 16*, 20811–20841. https://doi.org/10.1039/D4NR03543G

[5] Abbas, K., Ji, P., Ameer, M. F., & Yang, S. (2025). Enhanced photoresponse and stability in graphene/silicon Schottky photodetectors modified with perovskite nanoparticles. *Applied Surface Science, 714*, 164485.

[6] Wu, J.-Y., Jiang, H.-Y., Wen, Z.-Y., & Wang, C.-R. (2023). Fundamental and photodetector application of van der Waals Schottky junctions. *Adv. Devices Instrum., 4*, 0022.

[7] Tian, Y., Liu, H., Li, J., Liu, B., & Liu, F. (2025). Recent developments of advanced broadband photodetectors based on 2D materials. *Nanomaterials, 15*(6), 431.

[8] Delgado-Notario, J. A., Bray, C., Pérez-Martín, E., et al. (2025). Resonant Dyakonov–Shur magnetoplasmons in graphene terahertz photodetectors. *Nano Lett.*

[9] Yu, W., Zhao, L., Gao, Y., Gao, S., Yang, Y., Pan, C., Liang, S.-J., & Cheng, B. (2025). Gate-tunable high-responsivity photodiode based on 2D ambipolar semiconductor. *Chin. Phys. B, 34*(1), 018502.

[10] Wei, L., Wu, T., Cui, Q., Yuan, H., & Wang, S. (2025). Polarimetric photodetector with ultrahigh-sensitivity and polarity reverse based on quasi-1D semimetal $(TaSe_4)_2I$/2D $MoTe_2$ heterojunction. *Adv. Mater.*